Artificial hemoprotein nanotubes†

Gang Lu,[a] Teruyuki Komatsu*[ab] and Eishun Tsuchida*[a]

Received (in Cambridge, UK) 20th March 2007, Accepted 23rd April 2007
First published as an Advance Article on the web 9th May 2007
DOI: 10.1039/b704135g

Artificial hemoprotein nanotubes have been prepared by a layer-by-layer deposition technique with human serum albumin (HSA) incorporating the synthetic heme (FeP) [HSA–FeP] using an anodic porous alumina template; each of the liberated tubules has a very uniform outer/inner diameter and can reversibly bind dioxygen (O_2) at 25 °C.

Template-synthetic chemistry based on a layer-by-layer deposition technique using a nanoporous membrane has provided very uniform nanotubes composed of a variety of materials.[1–10] One of the successful examples is the beautiful hollow cylinders of poly(electrolyte)s, which are fabricated by alternate film forming within vertically oriented pore arrays of an anodic alumina template.[5,6a] Currently, it is a key challenge to confer a particular function on the nanotubes to enable their practical application. From this point of view, biomolecular poly(electrolyte)s, namely proteins and DNA, are very attractive molecules for the preparation of intelligent nanotubes due to their bioactivity, biocompatibility and chemical flexibility.[3b,c,6b]

Human serum albumin (HSA, Mw: 65 kDa) is a versatile protein in our blood plasma (4–5 g dL^{-1}) and acts as a transporter for a range of endogenous and exogenous compounds, such as fatty acids, bilirubin, thyroxine, hemin, and an abundance of drugs.[11,12] Recently, there has been intense interest in exploiting the non-specific binding property of HSA for the development of functional proteins.[13–15] We have demonstrated that a synthetic heme, 2-[8-{*N*-(2-methylimidazolyl)}octanoyloxymethyl]-5,10,15,20-tetrakis[{α,α,α,α-*o*-(1-methylcyclohexanamido)}phenyl]-porphinatoiron(II) (FeP, Scheme 1) is incorporated into HSA, and the formed artificial hemoprotein can reversibly coordinate dioxygen (O_2) under physiological conditions (pH 7.4, 37 °C) in a fashion similar to hemoglobin.[13] The saline solution of HSA–FeP has the potential to be an O_2-carrying plasma expander as a red blood cell substitute. On the other hand, HSA–Zn(II)protoporphyrin IX complex shows a long-lived photoexcited triplet state and acts as a sensitizer for the photoinduced reduction of water to hydrogen.[14] Gozin and co-workers reported the formation of stable HSA complexes with C_{60}-fullerene derivatives.[15] If one can universally prepare cylindrical hollow structures using the functional HSA having a synthetic active site, it will serve as a trigger to create a new class of protein nanotubes. Recombinant HSA is now manufactured on an industrial scale using yeast cells (*Pichia pastoris*),[16] which allows us to use the HSA nanotubes in biotechnology applications.

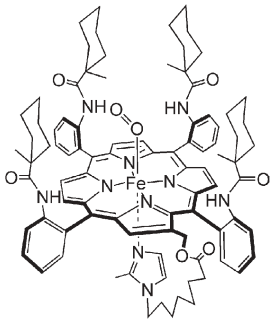

Scheme 1 Synthetic heme having an imidazolylalkyl-arm at the β-pyrrolic position of the porphyrin ring as a proximal base (FeP).

In this paper, we report for the first time the layer-by-layer fabrication of monodispersed nanotubes of HSA–FeP and highlight its O_2 binding properties (Scheme 2). The O_2 binding affinity of the nanotubes was 2-fold lower than that of the monomeric HSA–FeP, which was kinetically due to the low association rate constants.

Since the isoelectric point of HSA is unusually low (*p*I = 4.8), the protein forms a negatively charged heart-shape at a physiological pH 6–8 and a positively charged fast configuration at below pH 4.2.[11] The pH 3.8 and 7.0 solutions of the carbon monoxide (CO) adduct complex of HSA–FeP (FeP/HSA = 4, mol/mol) were alternately filtered through an anodic porous alumina membrane (Whatman Corp.) under reduced pressure. The layer-by-layer adsorption for three cycles of the oppositely charged HSA–FeP

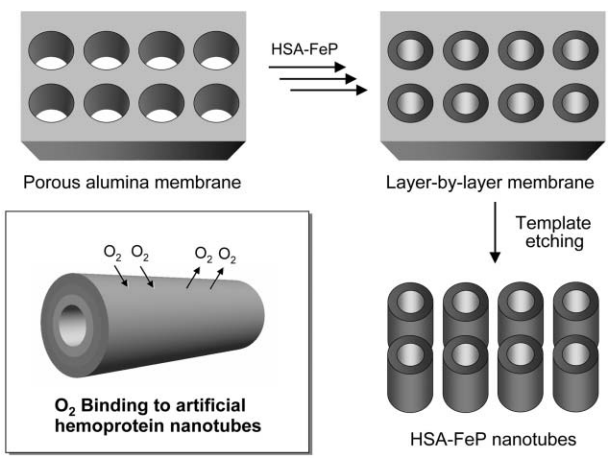

Scheme 2 Synthetic procedure for HSA–FeP nanotubes and schematic illustration of O_2 binding to nanotubes.

[a]*Advanced Research Institute for Science and Engineering, Waseda University, 3-4-1 Okubo, Shinjuku-ku, Tokyo 169-8555, Japan. E-mail: eishun@waseda.jp; teruyuki@waseda.jp; Fax: (+81) 3 3205 4740*
[b]*PRESTO, Japan Science and Technology Agency (JST), 4-1-8 Honcho, Kawaguchi-shi, Saitama 332-0012, Japan*
† Electronic supplementary information (ESI) available: Materials and experimental details. See DOI: 10.1039/b704135g

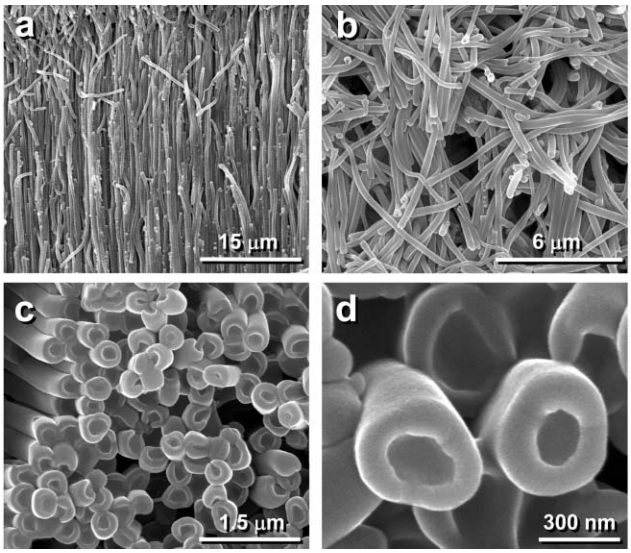

Fig. 1 Scanning electron microscopy observations of HSA–FeP nanotubes: a) micrometers length based on the template-synthesis, b) isolated and flexible structure, c) perpendicular orientation on the silicon wafer and the uniform outer/inner diameters, d) section of the nanotubes and very smooth surface.

produced a multi-layered film along the pore walls. The obtained red membrane was fixed on a silicon wafer or a quartz plate with epoxy resin and then immersed in 10% phosphoric acid to dissolve the alumina template (Scheme 2).

Scanning electron microscopy (SEM) images of the HSA–FeP nanotubes are shown in Fig. 1. The highly oriented nanotube arrays with a length of 60 μm are based on the template synthesis (Fig. 1a). Each of the tubules has a high flexibility and very uniform outer/inner (o/i) diameters (Fig. 1b,c). The averaged o/i values were determined to be 395 ± 23/186 ± 29 nm; the wall thickness was 104 ± 15 nm (Fig. 1d). Because the nanotubes were composed of 6 layers of HSA–FeP, one layer was estimated to be 17.3 nm, which is almost double the size of the HSA molecule (8 nm). This result was consistent with the expected value from the general principle of layer-by-layer membrane formation.[17] First, the positively charged molecules bind to the negative surface of the pore *via* electrostatic attraction. Since the surface charge is neutralised on the whole, further absorption of the excess molecules takes place and reverses the surface charge. The third sublayer cannot be formed because of the electrostatic repulsion. Then the next solution of the negatively charged molecules makes a new layer in the same manner. By repeating these cycles, an alternating multilayered cylinder was obtained. The elemental analysis of the HSA–FeP nanotubes by energy dispersive X-ray (EDX) spectroscopy showed the presence of C, N, O and Fe as membrane components.

For the transmission electron microscopy (TEM) observations, the red-colored anodic membrane with HSA–FeP was directly immersed in 10% phosphoric acid, and the liberated nanotubes were collected by filtration using a poly(carbonate) membrane. Although some of the tubes were damaged by the collection process, the TEM of the dried sample on a carbon-coated copper grid produced the same image of the nanotube with a diameter of 400 nm as the SEM measurements (Fig. 2). It is noteworthy that

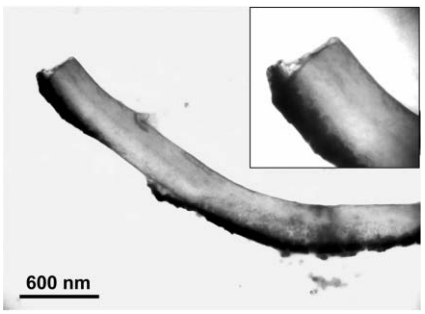

Fig. 2 Transmission electron microscopy observations of HSA–FeP nanotube. The dark stained cylinder implies that the negatively charged surface of the nanotube is coated by uranyl ions.

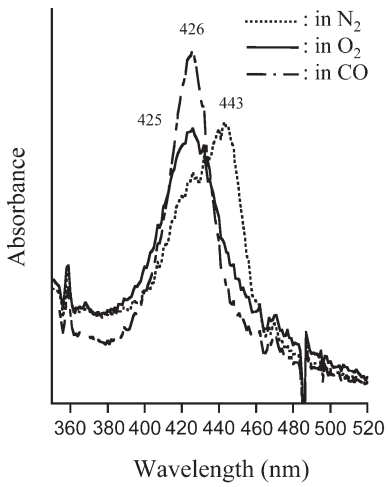

Fig. 3 UV–vis absorption spectral changes of HSA–FeP nanotubes on a quartz plate under various gaseous atmospheres at 25 °C.

the tubular surface was definitely stained dark by the contrast agent, uranyl acetate. This implies that divalent UO_2^{2+} strongly adhered to the negatively charged walls of the albumin nanotubes and that all the external surfaces of the cylinder were coated with uranyl ions.

The UV–vis absorption spectrum of the HSA–FeP nanotubes on a quartz plate showed a λ_{max} at 426 nm, indicating that the FePs are in the carbonyl complex (Fig. 3). After exposure to O_2 gas, the absorption intensity decreased and became slightly blue-shifted (λ_{max}: 425 nm). An N_2 flow for another several minutes changed the λ_{max} to 443 nm, indicating the formation of the five-N-coordinate ferrous complex of FeP.[13] This spectral change was repeated and found to be dependent on the O_2 partial pressure (0–760 Torr). We concluded that the HSA–FeP nanotubes can reversibly bind and release O_2 at 25 °C. The O_2 binding affinity ($P_{1/2}$: the O_2 partial pressure at which 50% FeP is dioxygenated) of the nanotubes could be directly determined by the gas flow technique.[13] The UV–vis absorption spectral changes at a different O_2 pressure gave a $P_{1/2}$ value of 26 Torr, which was 2-fold higher (lower O_2 binding constant K) than that of the monomeric HSA–FeP in phosphate buffered saline (PBS) solution (Table 1).

To evaluate the kinetics of O_2 and CO binding to the HSA–FeP nanotubes, laser flash photolysis experiments (Nd:YAG SHG; 532 nm; 5-ns pulse width) were carried out.[13,18] The time-course of

Table 1 O_2 and CO binding parameters of HSA–FeP nanotubes at 25 °C

HSA–FeP	$k_{on}^{O_2}$ ($Torr^{-1}$ s^{-1})	$k_{off}^{O_2}$ (s^{-1})	$P_{1/2}^{O_2}$ (Torr)	k_{on}^{CO} ($Torr^{-1}$ s^{-1})
Nanotubes[a]	7.2	184	26	1.9
Monomer[b,c]	51	530	13	5.1

[a] On a quartz plate. [b] In PBS solution (pH 7.4). [c] From ref. 13*b*. The k_{on} and k_{off} values of the major components of the binding reactions are represented. See note 19.

the absorbance change accompanying the O_2 or CO recombination to the HSA–FeP nanotubes after the laser pulse irradiation mostly followed a monophasic decay and showed a predominantly first-order kinetics (*ca.* 95%). The association rate constant for O_2 ($k_{on}^{O_2}$) was 7.1-fold lower than that of the monomeric HSA–FeP in PBS solution (Table 1).[19] The CO binding rate constant (k_{on}^{CO}) was also 2.9-fold lower compared to that of the monomer. The results are probably due to the slow diffusion of O_2 and CO gases within the multilayered assembly of the albumin to access the FePs.

We have demonstrated extremely uniform nanotubes made of artificial hemoprotein and their unique O_2 binding properties. The alternative layer-by-layer deposition technique with the very common blood protein, HSA, hybridized with the desired functional molecule, will lead to the development of a new field of smart nanotubes which can provide not only enhanced biological properties but also electronic, photonic, and/or magnetic performances. The photochemistry of fluorescent nanotubes made of HSA incorporating Zn(II)porphyrins or fullerenes is now under investigation.

This work was supported by PRESTO "Control of Structure and Functions", JST. G.L. is grateful for a JSPS Postdoctoral Fellowship for Foreign Researchers.

Notes and references

1 H. Masuda and K. Fukuoka, *Science*, 1995, **268**, 1466–1468.
2 (*a*) M. Steinhart, J. H. Wendorff, A. Greiner, R. B. Wehrspohn, K. Nielsch, J. Schilling, J. Choi and U. Gösele, *Science*, 2002, **296**, 1997; (*b*) M. Steinhart, R. B. Wehrspohn, U. Gösele and J. H. Wendorff, *Angew. Chem., Int. Ed.*, 2004, **43**, 1334–1344.
3 (*a*) S. Hou, C. C. Harrell, L. Trofin and C. R. Martin, *J. Am. Chem. Soc.*, 2004, **126**, 5674–5675; (*b*) S. Hou, J. Wang and C. R. Martin, *Nano Lett.*, 2005, **5**, 231–234; (*c*) S. Hou, J. Wang and C. R. Martin, *J. Am. Chem. Soc.*, 2005, **127**, 8586–8587.
4 Z. Liang, A. S. Susha, A. Yu and F. Caruso, *Adv. Mater.*, 2003, **15**, 1849–1853.
5 D. H. Kim, P. Karan, P. Göring, J. Leclaire, A.-M. Caminade, P. Majoral, U. Gösele, M. Steinhart and W. Knoll, *Small*, 2005, **1**, 99–102.
6 (*a*) S. Ai, G. Lu, Q. He and J. Li, *J. Am. Chem. Soc.*, 2003, **125**, 11140–11141; (*b*) G. Lu, S. Ai, Q. He and J. Li, *Langmuir*, 2005, **21**, 1679–1682.
7 M. Jin, X. Feng, L. Feng, T. Sun, J. Zhai, T. Li and L. Jiang, *Adv. Mater.*, 2005, **17**, 1977–1981.
8 J. Jang, S. Ko and Y. Kim, *Adv. Funct. Mater.*, 2006, **16**, 754–759.
9 C. Barrett, D. Iacopino, D. O'Carroll, G. De Marzi, D. A. Tanner, A. J. Quinn and G. Redmond, *Chem. Mater.*, 2007, **19**, 338–340.
10 H.-J. Wang, W.-H. Zhou, X.-F. Yin, Z.-X. Zhuang, H.-H. Yang and X.-R. Wang, *J. Am. Chem. Soc.*, 2006, **128**, 15954–15955.
11 T. Peters, *All about Albumin: Biochemistry, Genetics and Medical Applications*, Academic Press, San Diego, 1996.
12 (*a*) S. Curry, H. Madelkow, P. Brick and N. Franks, *Nat. Struct. Biol.*, 1998, **5**, 827–835; (*b*) J. Ghuman, P. A. Zunszain, I. Petitpas, A. A. Bhattacharya, M. Otagiri and S. Curry, *J. Mol. Biol.*, 2005, **353**, 38–52; (*c*) P. A. Zunszain, J. Ghuman, T. Komatsu, E. Tsuchida and S. Curry, *BMC Struct. Biol.*, 2003, **3**, 6.
13 (*a*) T. Komatsu, Y. Matsukawa and E. Tsuchida, *Bioconjugate Chem.*, 2002, **13**, 397–402; (*b*) Y. Huang, T. Komatsu, R.-M. Wang, A. Nakagawa and E. Tsuchida, *Bioconjugate Chem.*, 2006, **17**, 393–398.
14 T. Komatsu, R.-M. Wang, P. A. Zunszain, S. Curry and E. Tsuchida, *J. Am. Chem. Soc.*, 2006, **128**, 16297–16301.
15 B. Belgorodsky, L. Fadeev, J. Kolsenik and M. Gozin, *ChemBioChem*, 2006, **7**, 1783–1789.
16 K. Kobayashi, *Biologicals*, 2006, **34**, 55–59.
17 Y. Lvov, K. Ariga, I. Ichinose and T. Kunitake, *J. Am. Chem. Soc.*, 1995, **117**, 6117–6123.
18 (*a*) T. Komatsu, N. Ohmichi, A. Nakagawa, P. A. Zunszain, S. Curry and E. Tsuchida, *J. Am. Chem. Soc.*, 2005, **127**, 15933–15942; (*b*) T. Komatsu, Y. Matsukawa and E. Tsuchida, *Bioconjugate Chem.*, 2000, **11**, 772–776.
19 We have previously shown that the absorbance decays accompanying the O_2 and CO recombinations to HSA–FeP monomer [HSA/FeP = 1/4 (mol/mol)] in PBS solution were composed of double-exponential profiles [ratio of the fast and slow phases = 3/1].[13,18*b*] It was theorized that there are two different modes of the O_2 and CO binding process, *i.e.*, one of the four FePs may be accommodated in a deep crevasse of the protein and the O_2 binding to this FeP site appears to be sterically retarded.

